

## Nature of the Active Site in Surface-Enhanced Raman Scattering

T. E. Furtak and D. Roy

*Department of Physics, Rensselaer Polytechnic Institute, Troy, New York 12181*

(Received 21 January 1983)

Experiments involving competitive and cooperative adsorption of pyridine,  $\text{Cl}^-$ ,  $\text{SCN}^-$ , and Tl, and voltage induced resonance shifting show that the largest surface-enhanced Raman scattering intensity comes from complexes of these species adsorbed on defects which cover less than 3% of the Ag surface. The resonance is attributed to charge transfer excitation from Ag to pyridine and from  $\text{SCN}^-$  to Ag which is communicated to all vibrations of the complex.

PACS numbers: 78.30.Er, 34.70.+e

It has now been established that surface-enhanced Raman scattering (SERS) is caused, in part, by large local optical fields which are a by-product of the creation of surface plasmons in the rough metal substrate.<sup>1</sup> For the largest, frequently the only detectable levels of enhancement, a second, less clearly understood mechanism is simultaneously required. This mechanism is thought to be similar to the process which leads to the normal resonant Raman effect. When the incident photon energy,  $\hbar\omega$ , is equal to the excitation energy of an electronic transition within the system,  $\Delta E$ , then the Raman polarizabilities associated with many of the vibrational modes of the system are dramatically enhanced. This might occur if, upon adsorption, the molecular orbitals are replaced by hybrid metal-molecule states<sup>2</sup> and/or charge transfer excitations (CTE) become possible.<sup>3</sup> The latter concept has recently received strong support on the basis of electrochemical experiments in which  $\Delta E$  was shown to be a function of  $V_{\text{app}}$ , the externally applied metal-solution voltage.<sup>4,5</sup>

To clarify the role of CTE, its generality, and its relationship to previously hypothesized surface complexes<sup>6</sup> we have performed three types of experiments involving electrochemically controlled Ag in a supporting electrolyte of 0.1M NaCl. The  $\text{Cl}^-$  is required in the preparation of a properly "roughened" surface through the oxidation-reduction cycle (ORC). Two types of ORC were used. After the sample had been mechanically polished with 1- $\mu\text{m}$  abrasive the "external" ORC was performed in a nitrogen-purged 0.1M NaCl solution in a three-electrode electrochemical cell [ $-0.4$  to  $+0.2$  to  $-0.4$  V versus the saturated calomel reference electrode (SCE) at 0.3 V/min]. The activated sample was then transferred into a second cell within the Raman device, which is described elsewhere.<sup>5</sup> The second type of ORC was performed internally within the

same cell and solution in which the Raman data were acquired. In either case approximately 30 to 40  $\text{mC}/\text{cm}^2$  of charge was reformed in the ORC.

In each experiment the composition of the working solution can be characterized by 0.1M NaCl +  $X$ M NaSCN +  $Y$ M pyridine +  $Z$ M thallium acetate.

(1) *Competitive and cooperative adsorption and its effect on the surface complex which manifests itself in SERS.*—For this series  $X=0$ , 0.0001, 0.01, or 0.05;  $Y=0$  or 0.05; and  $Z=0$ . The external ORC was used. The object was to demonstrate how pyridine and  $\text{SCN}^-$ , each of which independently shows SERS, mutually affect each other on an active site which was created by an ORC performed in the absence of either molecule. The data are shown in Fig. 1.

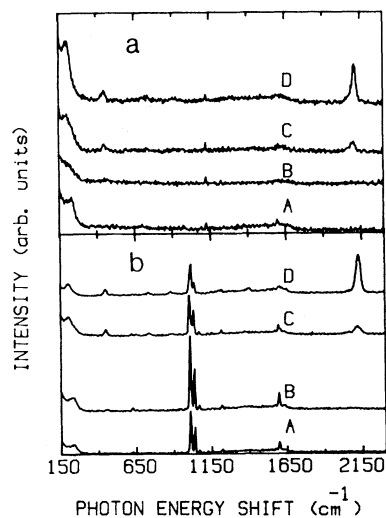


FIG. 1. Competitive adsorption in SERS in 0.1M NaCl,  $\hbar\omega=2.41$  eV, 140 mW,  $V_{\text{app}}=-0.4$  V (SCE),  $\Delta\nu=5$   $\text{cm}^{-1}$ , external ORC (a) without pyridine, (b) 0.05M pyridine. Curve A, no  $\text{SCN}^-$ ; curve B,  $10^{-4}$ M NaSCN; curve C,  $10^{-2}$ M NaSCN, curve D, 0.05M NaSCN.

From these results we see that pyridine and  $\text{Cl}^-$  or  $\text{SCN}^-$  are associated with each other on the active site. In part (a) of Fig. 1 we see how the Ag-Cl vibration at  $215\text{ cm}^{-1}$  is replaced, even for very low concentrations of NaSCN, by the Ag-SCN vibration at  $200\text{ cm}^{-1}$ . Part (b) shows that this replacement is inhibited when pyridine is present and does not take place until much higher concentrations of NaSCN are reached. The active site, which was originally stabilized by adsorbed  $\text{Cl}^-$  in the external ORC, immediately accepts either pyridine or  $\text{SCN}^-$ . However, when  $\text{SCN}^-$  is on the active site, it replaces  $\text{Cl}^-$  in the surface complex. When pyridine is present on the active site, the SERS intensities for vibrations of all the other residents on the active site increase.<sup>7</sup> [The data for Fig. 1(a) are multiplied by 4.5 compared to Fig. 1(b)]. The C-N stretch vibration ( $2105\text{ cm}^{-1}$ ) is stronger with pyridine [Fig. 1(b), curve D] than without pyridine [Fig. 1(a), curve D]. This shows how the influence of the resonance associated with pyridine is communicated to  $\text{SCN}^-$ , a clear indication that both are contained in the same surface complex.

(2) *Spontaneous and foreign-metal-induced loss of SERS activity.*—For this experiment  $X = 0$  or  $0.05$ ,  $Y = 0$  or  $0.05$ , and  $Z = 0$  or  $10^{-6}$ . The internal ORC was used before each run. The object was to show that the stabilities of pyridine and  $\text{SCN}^-$  on the active site are improved when both are present. In addition, the experiments were designed to show how thallium deposition, which destroys the enhancement,<sup>8</sup> identifies the type of surface site and its number density. After the ORC, the SERS intensities of several modes were recorded as functions of the time as shown in Fig. 2. Surface coverage of thallium was determined by stripping experiments to calibrate the surface area ( $4.86 \times$  geometrical area) and by standard application of diffusion-limited electrodeposition<sup>8</sup> (for our case  $\theta = 1.41 \times 10^{-4} \sqrt{t}$ ,  $t$  being time in seconds after the ORC). The time-dependent data of Fig. 2 further emphasize the association between pyridine and  $\text{SCN}^-$ . At  $V_{\text{app}} = -0.6\text{ V}$   $\text{SCN}^-$  is spontaneously desorbed over a period of time. However, when the complex is formed with pyridine this tendency is eliminated. This stability is characteristic of pyridine. The signal from the Ag-SCN vibration associated with pyridine stabilized by  $\text{Cl}^-$  also does not decay.

Further information on the stability of the complex is provided by the thallium deposition data (solid symbols). Although  $\text{Cl}^-$  stabilizes the active site with pyridine on it, comparison of the

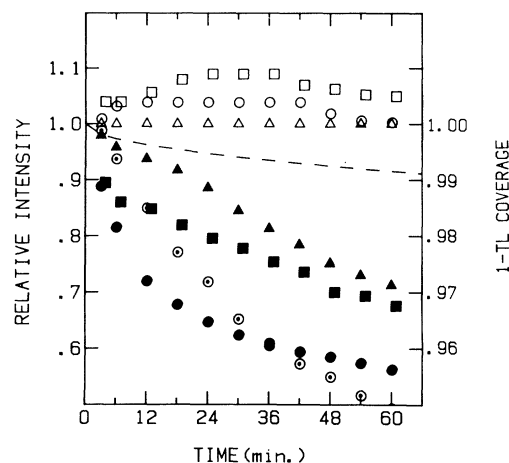


FIG. 2. Time dependence of relative SERS intensity in  $0.1M\text{ NaCl}$ ,  $\hbar\omega = 2.41\text{ eV}$ ,  $140\text{ mW}$ ,  $V_{\text{app}} = -0.6\text{ V}$  (SCE),  $\Delta\nu = 5\text{ cm}^{-1}$ , internal ORC. Open and dotted symbols, without  $\text{Tl}^+$ ; solid symbols, with  $10^{-6}M\text{ Tl}^+$ . Dot in circle,  $200\text{ cm}^{-1}$  Ag-SCN intensity in  $0.05M\text{ NaSCN}$  without pyridine; squares,  $0.05M$  pyridine. Circles,  $1008\text{ cm}^{-1}$  pyridine intensity without  $\text{SCN}^-$ ; triangles,  $0.05M\text{ NaSCN}$ . Dotted line is Tl coverage.

pyridine vibration in the presence of thallium shows that the signal decays faster without  $\text{SCN}^-$  (solid circles) than when the  $\text{Cl}^-$  in the complex is replaced by coadsorbed  $\text{SCN}^-$  (solid triangles). When the pyridine-thiocyanate-Ag complex is present on the active site, the thallium destroys the signal for pyridine (solid triangles) and for Ag-SCN (solid squares) at an equal rate. This reinforces the conclusion that the active sites are populated by both molecules and that the quenching is a characteristic of the interaction of thallium with the Ag rather than with either pyridine or  $\text{SCN}^-$ . This is not surprising since we know that thallium deposition occurs at a very high rate on surface defects (as opposed to deposition of Pb).<sup>9</sup>

In Fig. 2, note how 30% to 40% of the signal is destroyed with only 0.8% of the surface covered with thallium. This proves that the active sites on which the surface complex forms are associated with surface defects and that they cover less than 3% of the surface.<sup>10</sup>

(3) *Voltage-induced electronic resonance shifting.*—Here  $X = 0$  or  $0.05$ ,  $Y = 0$  or  $0.05$ , and  $Z = 0$ . As in our previous work<sup>5</sup> we have recorded the SERS intensity of characteristic modes as a function of  $V_{\text{app}}$  after the internal ORC. The object was to demonstrate the generality of CTE and to confirm its association with a surface complex. The results for the pyridine- $\text{Cl}^-$  system are

shown in Fig. 3 and for the pyridine- $\text{SCN}^-$  system in Fig. 4. The latter is a particularly well-defined system since recent differential capacitance experiments have shown that the surface coverage of  $\text{SCN}^-$  remains constant throughout the range of  $V_{\text{app}}$  used here.<sup>11</sup> In these data the important information resides in line shape rather than absolute intensity changes. The results are thus independent of optical variations between the two excitation sources.

The character of the resonance is consistent with the concept of CTE between states which experience different electrostatic potentials. As shown in Fig. 3(b), curve B and Fig. 3(c), curve B for resonance involving pyridine, the optimum value of  $V_{\text{app}}$  depends on  $\hbar\omega$  since  $\Delta E$  is a function of  $V_{\text{app}}$ . It is striking to observe, however, how the influence of this resonance is directly communicated to the Ag-Cl vibration as well. The shoulders in Fig. 3(b), curve A and Fig. 3(c), curve A are clearly correlated with the maximum in the pyridine vibration data, Fig. 3(b), curve B and Fig. 3(c), curve B. When pyridine is absent,

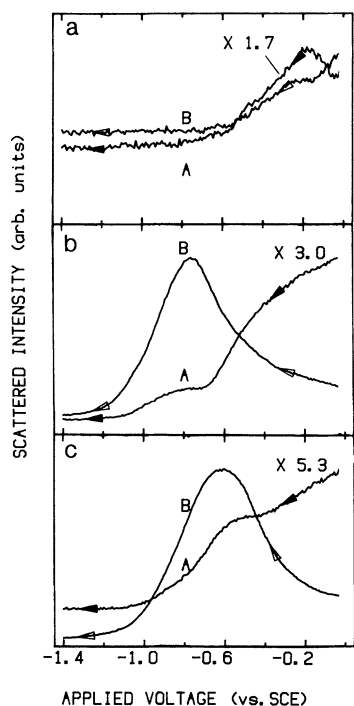


FIG. 3. Voltage-induced resonance shifting in 0.1M NaCl, 140 mW, internal ORC. (a)  $216\text{ cm}^{-1}$  Ag-Cl intensity vs  $V_{\text{app}}$  without pyridine, curve A,  $\hbar\omega = 1.92\text{ eV}$ ; curve B,  $\hbar\omega = 2.41\text{ eV}$ . (b)  $\hbar\omega = 1.92\text{ eV}$  with 0.05M pyridine; curve A,  $215\text{ cm}^{-1}$ ; curve B,  $1008\text{ cm}^{-1}$  pyridine intensity. (c)  $\hbar\omega = 2.41\text{ eV}$  with 0.05M pyridine; curves A and B, same as in (b).

Fig. 3(a), these shoulders are missing with both photon energies. Figure 3(a) also shows that the  $V_{\text{app}}$  dependence of the Ag-Cl vibration is not due to voltage-induced shifting of the molecular levels with respect to the metal as is the case with pyridine.

In contrast to the case of  $\text{Cl}^-$ ,  $\text{SCN}^-$  does demonstrate voltage-induced resonance shifting, as shown in Fig. 4(a). Here the resonance shifts in the opposite direction compared to pyridine. When  $\hbar\omega$  increases, the optimum  $V_{\text{app}}$  shifts to more negative values. Figures 4(b) and 4(c) show how the electronic resonances in each of these molecules are communicated to each other. There is an image of the pyridine resonance in the C-N vibration of  $\text{SCN}^-$  at negative values of  $V_{\text{app}}$  while the image of the  $\text{SCN}^-$  resonance appears in the pyridine vibration at more positive  $V_{\text{app}}$ . When  $\hbar\omega$  changes from 1.92 eV [Fig. 3(b)] to 2.41 eV [Fig. 4(c)] the resonant structures approach each other, since at larger  $\hbar\omega$  the optimum  $V_{\text{app}}$  for pyridine is at a more positive voltage while for  $\text{SCN}^-$  it is at a more negative voltage.

These data demonstrate that surface complexes involving pyridine and coadsorbed anions on a Ag surface defect are responsible for the electronic

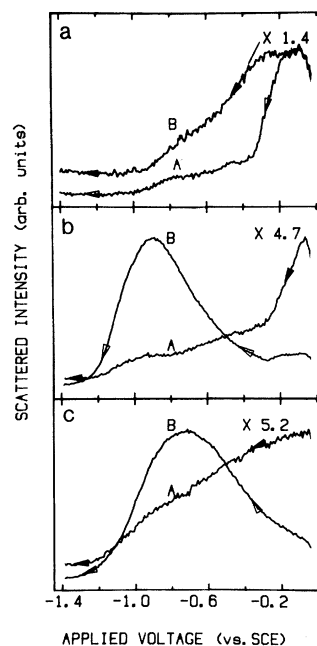


FIG. 4. Voltage-induced resonance shifting in 0.1M NaCl + 0.05M NaSCN. Same conditions as in Fig. 3. (a)  $2105\text{ cm}^{-1}$  C-N intensity vs  $V_{\text{app}}$  without pyridine; curve A,  $\hbar\omega = 1.92\text{ eV}$ ; curve B,  $\hbar\omega = 2.41\text{ eV}$ ; (b) and (c), same as in Fig. 3, except curve A is for  $2105\text{ cm}^{-1}$ .

component of SERS. We expect that CTE is the major contributor in this phenomenon. For pyridine the transition is from the Fermi level of Ag to a higher-energy empty state on the molecule. For  $\text{SCN}^-$  the transition is from a lower-energy filled state on the molecule to the Fermi level. The molecules are both located a short distance away from the metal and thus feel a different electrostatic potential than the metal. When  $V_{\text{app}}$  on the metal increases,  $\Delta E$  for metal to pyridine transition increases while  $\Delta E$  for  $\text{SCN}^-$  to metal transition decreases.

In addition to this influence on CTE,  $\Delta E$  is also a function of the perturbation which the adsorbed molecules experience due to orbital overlap with metal states. As the charge density on the metal surface changes in response to changes in  $V_{\text{app}}$  some of the voltage-induced resonance shift may be attributed to modification of the surface bond.

In the future it may be possible to control surface complex formation so as to provide enhancement on substrates such as Fe and Ni which are unfavorable with regard to their ability to support surface plasmon resonances. On favorable substrates (Ag, Au, Cu, Li, Al) it should still be possible to observe enhancement under optical resonance alone provided the contribution from

the electronic resonance due to minority surface complexes can be separated from the total signal.

Thanks are extended to B. Pettinger, A. Otto, T. Watanabe, and M. Weaver for preprints and to R. Messmer and S. Macomber for useful discussions. This work was supported by the U. S. Department of Energy, Office of Basic Energy Sciences.

---

<sup>1</sup>*Surface Enhanced Raman Scattering*, edited by R. K. Chang and T. E. Furtak (Plenum, New York, 1982).

<sup>2</sup>T. K. Lee and J. L. Birman, in Ref. 1, p. 51.

<sup>3</sup>K. Arya and R. Zeyher, *Phys. Rev. B* **24**, 1852 (1981).

<sup>4</sup>J. Billman and A. Otto, *Solid State Commun.* **44**, 105 (1982).

<sup>5</sup>T. E. Furtak and S. H. Macomber, to be published.

<sup>6</sup>B. Pettinger, M. R. Philpott, and J. G. Gordon, *J. Chem. Phys.* **74**, 934 (1981).

<sup>7</sup>H. Wetzel, H. Gerischer, and B. Pettinger, *Chem. Phys. Lett.* **78**, 392 (1981).

<sup>8</sup>T. Watanabe, N. Yanagihara, K. Honda, and B. Pettinger, to be published.

<sup>9</sup>M. Klimmeck and K. Jüttner, *Electrochim. Acta* **27**, 83 (1982).

<sup>10</sup>L. Moerl and B. Pettinger, *Solid State Commun.* **43**, 315 (1982).

<sup>11</sup>J. T. Hupp, D. Larkin, and M. J. Weaver, to be published.